Origin of the slow dynamics and the aging of a soft glass

Sylvain Mazoyer, Luca Cipelletti, Laurence Ramos

Origin of the slow dynamics and the aging of a soft glass

Sylvain Mazoyer, Luca Cipelletti and Laurence Ramos*
*Laboratoire des Colloïdes, Verres et Nanomatériaux (UMR CNRS-UM2 5587), CC26, Université Montpellier 2, 34095 Montpellier Cedex 5, France**
(Dated: March 28, 2006)

We study by light microscopy a soft glass consisting of a compact arrangement of polydisperse elastic spheres. We show that its slow and non-stationary dynamics results from the unavoidable small fluctuations of temperature, which induce intermittent local mechanical shear in the sample, because of thermal expansion and contraction. Temperature-induced shear provokes both reversible and irreversible rearrangements whose amplitude decreases with time, leading to an exponential slowing down of the dynamics with sample age.

PACS numbers: 82.70.-y, 61.20.Lc, 61.43.-j, 62.20.Fe

Quite generally, correlation functions in glassy systems exhibit a two-step relaxation [1]. This applies to supercooled molecular liquids and spin glasses, but also to a large variety of soft materials, such as concentrated colloidal suspensions [2], emulsions [3], surfactant phases, and gels [4]. In soft glasses, the initial decay of density-density correlators measured e.g. by dynamic light scattering is well understood: it corresponds to the thermally activated motion of particles in the cage formed by their neighbors [2], or to overdamped phonons, whose amplitude is restricted by structural constraints, like in concentrated emulsions [3] or surfactant phases [4]. By contrast, the motion associated with the final relaxation of the correlation function is still poorly understood, in spite of the large research effort of the last years. Subdiffusive [2, 5], diffusive [6], hyperdiffusive [7] and ballistic [4, 8] behavior has been observed, often associated with dynamical heterogeneity [9, 10, 11, 12] and aging [5, 6, 7, 13, 14]. In most cases, the origin of this slow dynamics is not clear, although elasticity and the relaxation of internal stress have been highlighted as possible key ingredients [4, 7, 8, 15]. Indeed, light scattering experiments coupled to rheology have shown that an external oscillatory shear strain can help the system evolve towards a more relaxed configuration, presumably by relaxing internal stress [13, 16, 17]. However, the physical mechanism by which internal stress may be relaxed in undriven systems has not been identified clearly to date.

In this Letter we present time- and space-resolved light microscopy experiments that probe the aging dynamics of a soft glass made of a compact arrangement of elastic spheres. Surprisingly, we find that the driving mechanism for the slow evolution of the sample configuration are the experimentally unavoidable fluctuations of temperature, which induce intermittent local mechanical shears in the sample, due to thermal expansion and contraction. We find that the amplitude of both reversible and irreversible rearrangements provoked by the shear decreases with time, leading to aging.

The experimental system has been described in detail elsewhere [18]. The sample is a dense packing (volume fraction 1) of polydisperse multilamellar vesicles, or onions. The radius of the largest onions is about $6\,\mu$m. Each onion consists of a regular stack of concentric surfactant bilayers in salted water ([NaCl] = 0.2M) at 16% weight fraction. Bilayers are composed of a mixture of cetylpyridinium chloride (CpCl), octanol (Oct) and Symperonics F68 by Serva, an amphiphilic copolymer of formula $(EO)_{76} - (PO)_{29} - (EO)_{76}$, where EO is ethylene oxide and PO is propylene oxide. The weight ratios are CpCl/Oct = 0.95 and F68/(CpCl + Oct) = 0.8. Because of the temperature dependence of the hydrophobicity of F68, the sample is fluid at 5°C and gel-like at room temperature [18]. Previous rheology and dynamic light scattering experiments [15, 19] have shown that this system displays a slow dynamics that slows down as the sample ages following an inverse temperature quench from the fluid to the gel-like phase.

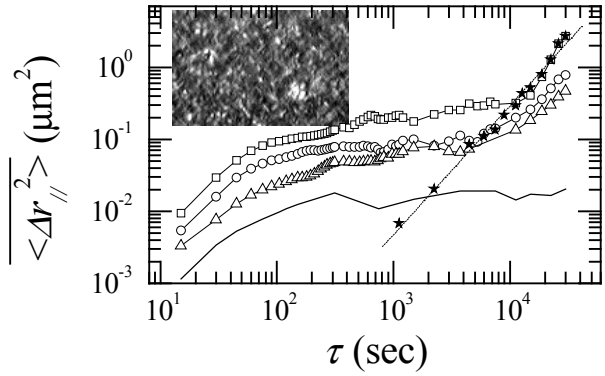

FIG. 1: (Open symbols) Mean squared relative displacement (MSD) along the long axis of the capillary as a function of the time lag τ. The sample age is $t_w = 7500$ sec (squares), 22500 sec (circles) and 37500 sec (triangles). Stars: MSD calculated by taking into account only the irreversible rearrangements. The dotted line is a power law fit yielding an exponent 1.8 ± 0.1. Full line: "mean squared displacement" of the temperature fluctuations, $\overline{(\Delta T)^2}$, as defined in the text. Inset: Portion of a typical light microscopy image of the onion sample of size $283\,\mu\text{m} \times 184\,\mu\text{m}$.

The sample is loaded at 5°C in a glass capillary of

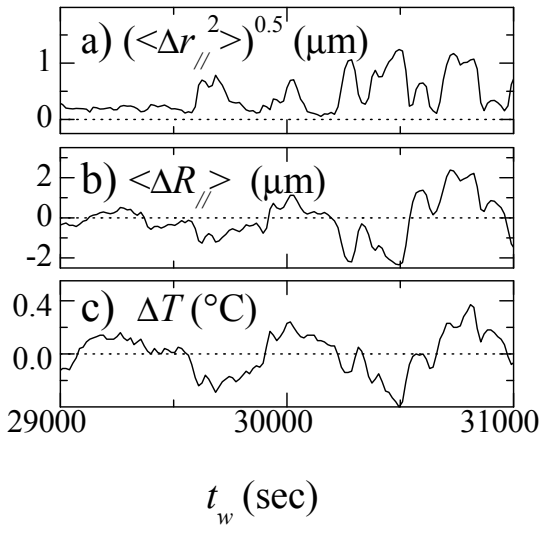

FIG. 2: Age dependence of a) the square root relative parallel displacement, $\sqrt{\langle \Delta r_\parallel(t_\mathrm{w},\tau)^2\rangle}$; b) the global parallel displacement $\langle \Delta R_\parallel(t_\mathrm{w},\tau)\rangle$; c) the temperature fluctuations $\Delta T(t_\mathrm{w},\tau)$. In all panels, the lag is $\tau = 315$ sec.

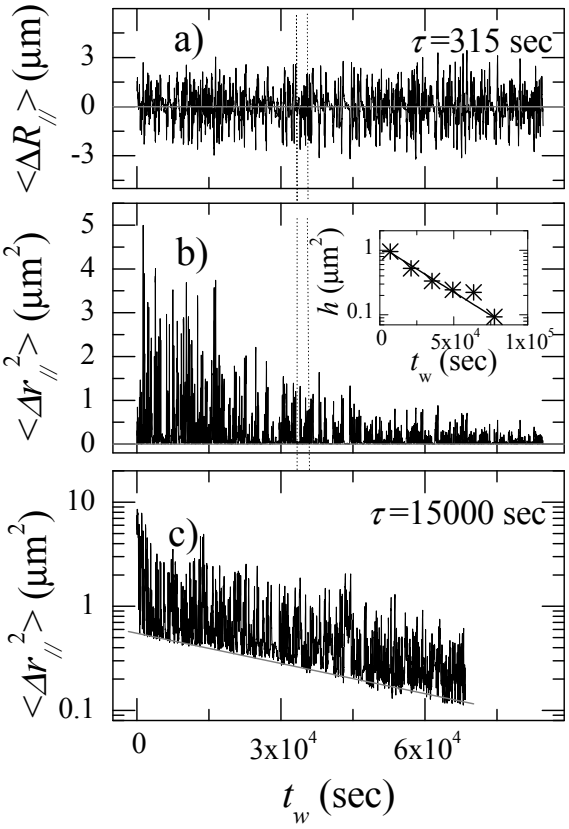

FIG. 3: Age dependence of a) the spatially-averaged absolute displacement at a lag $\tau = 315$ sec; b) and c) the relative squared displacement at lags $\tau = 315$ and 15000 sec, respectively. The vertical dotted lines in a) and b) show the time window expanded in figs. 2 a) and b). The finite base line in c) (grey line) corresponds to irreversible rearrangements that persist even when $\Delta T = 0$. Inset of b): mean value of the top 25% intermittent peaks of $\langle \Delta r_\parallel^2\rangle$ as a function of sample age (symbols); the line is an exponential fit.

length a few cm and rectangular cross-section ($0.2 \times 2\,\mathrm{mm}^2$), which is flame-sealed to prevent evaporation. Centrifugation is used to confine the air bubble left after filling at one end of the capillary. The sample is then placed in an oven (Instec) that sets the temperature T to 20 ± 0.15°C (T is measured on the capillary in the close vicinity of the sample). A microscope equipped with a 10x objective is used to image the onions between crossed polarizers (Part of an image is shown in the inset of Fig. 1). The field of view is $0.93\,\mathrm{mm} \times 1.24\,\mathrm{mm}$ and is located in the center of the capillary. Images are taken every 15 sec for about 24 hours, after initializing the dynamics by a T jump from 5°C to 20°C. Age $t_w = 0$ is defined as the time at which T has reached 20°C. We use a technique derived from Particle Imaging Velocimetry [20] to quantify the time evolution of the displacement field. Each image is divided into 192 regions of interest (ROIs) corresponding to $76\,\mu\mathrm{m} \times 76\,\mu\mathrm{m}$ in the sample and the displacement $\Delta\mathbf{R}_i(t_w,\tau)$ of each ROI for pairs of images taken at time t_w and $t_\mathrm{w} + \tau$ is measured. The experimental uncertainty is 3×10^{-2} pixel; thus, displacements as small as 50 nm can be measured over a field of view larger than 1 mm.

We first discuss the relative displacement, defined as $\Delta\mathbf{r}_i(t_w,\tau) = \Delta\mathbf{R}_i(t_\mathrm{w},\tau) - \langle\Delta\mathbf{R}_i(t_\mathrm{w},\tau)\rangle$, where $\langle\cdots\rangle$ denotes an instantaneous spatial average over all ROIs. We calculate the mean-squared relative displacements (MSDs) $\overline{\langle\Delta r_\parallel(t_w,\tau)^2\rangle}$ and $\overline{\langle\Delta r_\perp(t_w,\tau)^2\rangle}$, where the subscript i has been dropped for simplicity and $\parallel$ and $\perp$ refer to the two horizontal components of $\Delta\mathbf{r}_i$, parallel and perpendicular to the long axis of the capillary, respectively. $\overline{\cdots}$ denotes a time average over a window of 15000 sec centered around t_w. We find that the motion is strongly anisotropic, with the parallel displacement typically one order of magnitude larger than the perpendicular one; therefore, in the following we focus on the parallel motion that dominates the dynamics. Figure 1 shows the parallel MSD as a function of the lag τ, for three ages (open symbols). Three distinct regimes are observed: a first rapid increase of the MSD with τ at short lags, an almost flat plateau at intermediate lags, extending over about two orders of magnitude in τ, and a long-lag regime where the MSD increases again strongly with τ. Moreover, the dynamics slows down with age, as revealed unambiguously by the decrease of the MSD with t_w at all lags.

To get insight in the physical mechanisms at the origin of this slow dynamics, we examine time-resolved quantities. The two-time squared relative displacement, $\langle\Delta r_\parallel(t_\mathrm{w},\tau)^2\rangle$, exhibits strong fluctuations with t_w, with intermittent peaks of high amplitude. This is shown, for $\tau = 315$ sec, in fig. 2a for a short time window and in

fig. 3b for the whole duration of the experiment (this lag corresponds to the plateau of the MSD, see fig. 1). A visual inspection of the movie of the sample motion suggests that the fluctuations of the relative displacement are associated with those of the global displacement, $\langle \Delta R_{\parallel}(t_w,\tau)\rangle$, and that the latter are of the same order of magnitude as the former. The movie shows also a large drift during the initial temperature jump, due to the thermal expansion of the sample. This suggests that the fluctuations of $\langle \Delta R_{\parallel}\rangle$ recorded once a constant temperature is reached may be due to small fluctuations of T, which are experimentally unavoidable. Indeed, a raise (decrease) of T would induce an expansion (contraction) of the sample. Because the material is confined in a capillary, it would deform essentially perpendicular to the free interface. Hence, the expansion/contraction of the sample is expected to be uniaxial, resulting mostly in a global displacement in the $\parallel$ direction, as observed experimentally.

To test this hypothesis, we show in fig. 2c the fluctuations of the temperature, defined as $\Delta T(t_w,\tau) = T(t_w+\tau) - T(t_w)$, and we compare them to $\sqrt{\langle \Delta r_{\parallel}^2(t_w,\tau)\rangle}$ (fig. 2a) and $\langle \Delta R_{\parallel}(t_w,\tau)\rangle$ (fig. 2b). Clearly, whenever ΔT increases or decreases so does $\langle \Delta R_{\parallel}\rangle$. Similarly, any peak in the relative mean squared displacement (positive by definition) corresponds to a (positive or negative) fluctuation of ΔT. Note that although temperature fluctuations result in an intermittent back and forth motion, the time-averaged value of the global displacement $\langle \Delta R_{\parallel}\rangle$ is 0 (see fig. 3a), consistently with the fact that there is no net drift of T. The similarity between the different signals shown in fig. 2 can be quantified by calculating their linear correlation coefficient, c, which ranges from 0 (for uncorrelated quantities) to 1 (for perfectly correlated quantities). For the pair $\Delta T(t_w)$, $\langle \Delta R_{\parallel}(t_w)\rangle$ and for all ages, we find $c \simeq 0.65$ demonstrating a strong correlation between the fluctuations of the global displacement field and those of the temperature. A significant correlation, although with a lower value $c \simeq 0.36$, is also found between $\sqrt{\Delta T^2}$ and $\sqrt{\langle \Delta r_{\parallel}^2\rangle}$, suggesting that the larger the global displacement field, the more spatially heterogeneous the deformation. This heterogeneity is in contrast to what may be expected for simple fluids or diluted suspensions. It is likely to stem from local variations of the viscoelastic properties of the sample, due to its jammed nature, and to the curvature of the meniscus at the sample-air interface. We find that, for lags corresponding to the MSD plateau, the relative displacement field most often corresponds to a shear in the parallel direction, as shown in fig. 4. Note that the displacement field varies slowly: thus, the dynamics is strongly correlated in space and the shear, of order 0.1% at most, is moderate and well in the linear regime, as checked by rheology experiments.

To seek further support for the crucial role of temperature fluctuations in driving the sample deformation, we compare the macroscopic thermal expansion coefficient of the onions, χ_T, to that estimated from the microscope observations. For the latter, one has $\chi_T = \frac{1}{L}\frac{\delta L}{\delta T}$, where $L = 2$ cm is the length of the sample from the bubble-free capillary end to the position of the field of view and δL the length variation provoked by a temperature variation δT. To estimate $\delta L/\delta T$, we take for δT the standard deviation of $\Delta T(t_w,\tau)$, and for δL the standard deviation of the absolute displacement, $\langle \Delta R_{\parallel}(t_w,\tau)\rangle$. Using the data for $\tau = 315$ sec, we find $\chi_T = (4 \pm 1)\times 10^{-4}/^{\circ}$C in good agreement with $2.6\times 10^{-4}/^{\circ}$C for water [21].

Temperature fluctuations are thus at the origin of the intermittent motion shown in figs. 3a and 3b, where peaks of ΔT correspond to large fluctuations of $\langle \Delta R_{\parallel}(t_w,\tau)\rangle$ and hence of $\langle \Delta r_{\parallel}^2\rangle$. Given the key role of temperature fluctuations, deeper insight on the evolution of the MSD shown in fig. 1 may be obtained by comparing the $\langle \Delta r_{\parallel}^2\rangle$ data to the analogous of the MSD for T, $f_T(\tau) = \overline{\Delta T(t_w,\tau)^2}$. This quantity is plotted in fig. 1 as a solid line and displays remarkable analogies with the MSD. Similarly to the MSD, $f_T(\tau)$ increases with τ until reaching a plateau for $\tau = \tau_c \sim 300$ sec, a time scale of the order of the slowest fluctuations of T. For τ smaller than τ_c, the temperature is on average monotonic. The relative MSD follows the evolution of T and hence increases monotonically as well. By contrast, for time lags $\tau \gtrsim \tau_c$, the sample has been submitted to several positive and negative fluctuations of ΔT, which have induced several shear deformations in the two opposite directions. On these time scales, this back and forth motion is virtually fully reversible and does not lead to a growth of the cumulated displacement; hence, a plateau is measured for the MSD. The reversible nature of the motion in this regime is further supported by the observation that the peaks of two-time squared displacement shown in fig. 3b raise from a base line that is essentially zero, corresponding to pairs of images taken —by chance— at nearly the same temperature. Thus, the initial growth of $\langle \Delta r_{\parallel}^2\rangle$ and the plateau are not due to the usual "rattling in the cage" mechanism, but rather to reversible shear deformations caused by temperature fluctuations. However, while $f_T(\tau)$ saturates at the plateau value for all $\tau > \tau_c$, a further increase of the MSD is observed at very large τ. This suggests that the expansion/contraction cycles imposed by the fluctuations of T eventually lead to significant irreversible rearrangements, whose cumulated effect is responsible for the final growth of the MSD.

This picture is confirmed by the time evolution of $\langle \Delta r_{\parallel}^2(t_w,\tau)\rangle$ calculated for a lag $\tau = 15000\,\mathrm{sec} \gg \tau_c$ and shown in fig. 3c. Intermittent peaks similar to those of fig. 3b are observed, corresponding to the largest values of $\Delta T(t_w,\tau)$. In contrast with the data for shorter lags, however, the peaks in fig. 3c raise from a base line larger than zero (grey line). As discussed previously, the base-

line corresponds to pairs of images taken at nearly the same T, in the absence of any global displacements. A non-zero baseline confirms that the temperature-induced shear deformations have led to irreversible rearrangements of the sample. This behavior is reminiscent of microscopy and echo dynamic light scattering experiments on concentrated suspensions of hard spheres and emulsions [16, 17, 22]. In these experiments, an oscillatory strain is mechanically imposed to the sample whose evolution is monitored by comparing the system configuration at each cycle. Repeated deformations lead to irreversible rearrangements, provided that the strain is larger than a critical value that decreases as jamming is approached [22]. In our experiments no mechanical shear is imposed; remarkably, however, the small strain $\sim 10^{-3}$ due to temperature fluctuations $\delta T \sim 0.1°$C is sufficient to induce irreversible rearrangements on very long time scales. At a given age, the height of the baseline shown in fig. 3c provides a direct measurement of the relative mean squared displacement for $\tau = 15000$ sec when only irreversible rearrangements are taken into account. We calculate the irreversible mean squared displacement, $\mathrm{MSD_{irr}}(\tau)$, by analyzing in a similar way data at a variety of time lags, and show in fig. 1 the result for $t_\mathrm{w} = 7500$ sec (star symbols). Remarkably, we find $\mathrm{MSD_{irr}} \sim \tau^\mathrm{p}$ over more than two orders of magnitude in τ, with $p = 1.8 \pm 0.1$, thus indicating that the irreversible motion is close to ballistic, for which $p = 2$. We stress that a similar ballistic motion has been invoked to explain the slow dynamics in a variety of soft glassy materials probed by light and X-photon scattering techniques [4, 8, 19], including the very same samples described here.

With age, the change in configuration corresponding to both the reversible and the irreversible rearrangements diminishes: this is demonstrated by the decrease of the height of the peaks of $\langle \Delta r_\parallel^2 \rangle$ with t_w (figs. 3b and c), as well as by the negative slope of the base line of $\langle \Delta r_\parallel^2 \rangle$ measured at long lags (fig. 3c). We find that the amplitude of both reversible and irreversible rearrangements decays exponentially with sample age, with roughly the same characteristic time τ_aging: independently of τ, we find $\tau_\mathrm{aging} \sim 39900 \pm 5500\,(30200 \pm 4300)$ sec for irreversible (reversible) rearrangements. For irreversible rearrangements, τ_aging is obtained from the slope of the base line in a log-lin representation of $\langle \Delta r_\parallel^2 \rangle$ *vs* t_w, as in fig. 3c. For reversible rearrangements, we divide the data in 6 time windows and plot the average height, h, of the top 25% largest peaks of each window as a function of sample age (see inset of fig. 3b); τ_aging is then obtained by fitting an exponential decay to $h(t_\mathrm{w})$ [23]. A similar exponential aging has been observed for other soft glasses [4, 6]; it may be explained by assuming $\mathrm{MSD_{irr}} \propto \mathrm{n_{rearr}}$, where n_rearr is the number of irreversible rearrangements per unit time, occurring in "weak sites". These sites correspond to the regions that are initially most unstable mechanically and are more likely to be relaxed by a rearrangement. We further assume $n_\mathrm{rearr} = \Gamma N(t)$, with Γ the probability of rearrangement per unit time (dictated by the fluctuations of temperature and thus independent of age) and $N(t)$ the number of weak sites not yet rearranged. The temporal evolution of N obeys $dN(t)/dt = -\Gamma N(t)$ and hence $N(t) \propto \exp(-\Gamma t)$, thus explaining the exponential decay of the irreversible mean square displacement. Note that the amplitude of the deformation field due to a temperature-induced expansion or contraction is likely to be larger the more numerous the weak zones still to be relaxed. Thus, the evolution of $N(t)$ would also explain the exponential decay of h that parallels that of $\mathrm{MSD_{irr}}$.

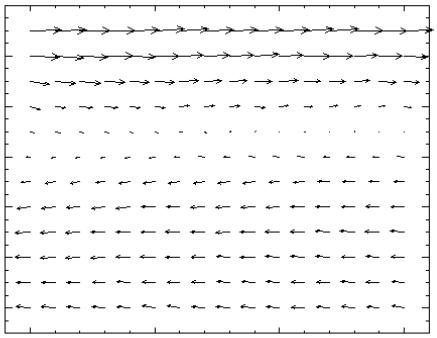

FIG. 4: Relative displacement field between two images separated by 315 sec. The arrows indicate the displacement for each ROI. The size of the images is 0.93 mm × 1.24 mm. The age of the sample is 2280 sec. Factor 200.

As a final remark, we note that our sample, although a priori at rest, is in fact mechanically driven (by T fluctuations) and as such presents analogies with colloidal systems submitted to mechanical shear [13, 16, 17, 24] or vibrated granular media [25]. The behavior reported in this work should be quite general in all soft systems where elasticity prevails over dissipation and whose constituents are closely packed, e.g. in concentrated emulsions or surfactant phases.

We thank W. Kob, L. Berthier, E. Pitard for discussions. This work was supported in part by the European MCRTN "Arrested matter" (MRTN-CT-2003-504712) and NOE "SoftComp" (NMP3-CT-2004-502235), and by CNES (03/CNES/4800000123) and the Ministère de la Recherche (ACI JC2076). L.C. is a junior member of the Institut Universitaire de France.

* Electronic address: ramos@lcvn.univ-montp2.fr

[1] E. Donth, *The Glass Transition* (Springer, Berlin, 2001).
[2] W. van Megen *et al.* Phys. Rev. E **58**, 6073 (1998).
[3] H. Gang *et al.*, Phys. Rev. E **59**, 715 (1999).
[4] L. Cipelletti *et al.*, Faraday Discuss. **123**, 237 (2003).

[5] N. B. Simeonova and W. K. Kegel, Phys. Rev. Lett. **93**, 035701 (2004).
[6] B. Abou, D. Bonn and J. Meunier, Phys. Rev. E **64**, 021510 (2001).
[7] A. Knaebel *et al.*, Europhys. Lett. **52**, 73 (2000).
[8] R. Bandyopadhyay *et al.* Phys. Rev. Lett. **93**, 228302 (2004).
[9] W. K. Kegel and A. van Blaaderen, Science **287**, 290 (2000).
[10] E. R. Weeks *et al.*, Science **287**, 627 (2000).
[11] L. Cipelletti *et al.*, J. Phys.: Condens. Matter **15**, S257 (2003).
[12] A. Duri *et al.*, Phys. Rev. E **72**, 051401 (2005).
[13] V. Viasnoff and F. Lequeux, Phys. Rev. Lett. **89**, 065701 (2002).
[14] R. E. Courtland and E. R. Weeks, J. Phys.: Condens. Matter **15**, S359 (2003).
[15] L. Ramos and L. Cipelletti, Phys. Rev. Lett. **94**, 158301 (2005).
[16] P. Hébraud *et al.*, Phys. Rev. Lett. **78**, 4657 (1997).
[17] G. Petekidis, A. Moussaïd and P. N. Pusey, Phys. Rev. E **66**, 051402 (2002).
[18] L. Ramos *et al.*, Europhys. Lett. **66**, 888 (2004).
[19] L. Ramos and L. Cipelletti, Phys. Rev. Lett. **87**, 245503 (2001).
[20] P. T. Tokumaru and P. E. Dimotakis, Experiments in Fluids **19**, 1 (1995).
[21] Recall that the onion phase is composed by 84% water.
[22] D. J. Pine *et al.*, Nature **438**, 997 (2005).
[23] Similar results are obtained with other threshold values.
[24] F. Ozon *et al.*, Phys. Rev. E **68**, 032401 (2003).
[25] E. R. Novak *et al.*, Phys. Rev. E **57**, 1971 (1998).